



AMERICAN METEOROLOGICAL SOCIETY

Bulletin of the American Meteorological Society

EARLY ONLINE RELEASE

This is a preliminary PDF of the author-produced manuscript that has been peer-reviewed and accepted for publication. Since it is being posted so soon after acceptance, it has not yet been copyedited, formatted, or processed by AMS Publications. This preliminary version of the manuscript may be downloaded, distributed, and cited, but please be aware that there will be visual differences and possibly some content differences between this version and the final published version.

The DOI for this manuscript is doi: 10.1175/BAMS-D-14-00136.1

The final published version of this manuscript will replace the preliminary version at the above DOI once it is available.

If you would like to cite this EOR in a separate work, please use the following full citation:

Carbin, G., M. Tippett, S. Lillo, and H. Brooks, 2015: Visualizing Long-range Severe Thunderstorm Environment Guidance from CFSv2. Bull. Amer. Meteor. Soc. doi:10.1175/BAMS-D-14-00136.1, in press.

© 2015 American Meteorological Society



Bulletin of the American Meteorological Society

Visualizing Long-range Severe Thunderstorm Environment Guidance from CFSv2

Gregory W. Carbin, Michael K. Tippett, Samuel P. Lillo, Harold E. Brooks

AFFILIATIONS:

Carbin — NOAA/NWS, Storm Prediction Center, Norman, OK

Tippett — International Research Institute for Climate and Society, Columbia University,
New York, NY

Lillo — Cooperative Institute of Mesoscale Meteorological Studies (CIMMS), University
of Oklahoma, Norman, OK

Brooks — NOAA/OAR/National Severe Storms Laboratory, Norman, OK

CORRESPONDING AUTHOR:

Gregory Carbin

NOAA/NWS Storm Prediction Center

120 David L. Boren Blvd. Norman, OK

73072

(405) 249-5313 E-mail: gregory.carbin@noaa.gov.

1 Capsule

2 The Climate Forecast System (CFSv2) is used to demonstrate new methods of
3 visualizing large sets of model forecasts, with the application of extended-range
4 forecasts for environments conducive to severe thunderstorms.

5

6 Abstract

7 Two novel approaches to extending the range of prediction for environments conducive
8 to severe thunderstorm events are described. One approach charts Climate Forecast
9 System version 2 (CFSv2) run-to-run consistency of the areal extent of severe
10 thunderstorm environments using grid counts of the Supercell Composite Parameter
11 (SCP). Visualization of these environments is charted for each 45-day CFSv2 run
12 initialized at 0000 UTC. CFSv2 ensemble mean forecast maps of SCP coverage over
13 the contiguous United States are also produced for those forecasts meeting certain
14 criteria for high impact weather. The applicability of this approach to the severe weather
15 prediction challenge is illustrated using CFSv2 output for a series of severe weather
16 episodes occurring in March and April 2014. Another approach, possibly extending
17 severe weather predictability from CFSv2, utilizes a run-cumulative time-averaging
18 technique of SCP grid counts. This process is described and subjectively verified with
19 severe weather events from early 2014.

20

INTRODUCTION

After violent tornadoes across the South and Midwest United States in 2011 and 2012, questions arose as to whether the National Oceanic and Atmospheric Administration (NOAA) National Weather Service (NWS) could provide seasonal severe thunderstorm outlooks analogous to seasonal hurricane outlooks (WMO 2007). While NOAA provides climatological information of severe weather through its National Storm Prediction Center (SPC) and National Center for Environmental Information (NCEI), as well as monthly and seasonal temperature and precipitation outlooks from the Climate Prediction Center (CPC), severe thunderstorm forecasts beyond eight days are not part of any operational product suite. However, emerging science suggests that low-frequency (time-scales of a week to months) modes of climate variability (e.g., the Pacific-North American Pattern) may modulate severe weather activity and severe weather environments (Allen et al. 2015, Tippett et al. 2015). Given these relationships, if forecast models are able to simulate such low-frequency modes of variability, they may also be able to capture the modulation of severe weather environments, and thereby provide extended-range guidance for severe weather activity. A particular challenge of severe weather is that it occurs on short time scales, unlike persistent climate phenomena such as drought. Consequently, model guidance for severe weather needs to contain information about severe weather environments on daily or shorter time scales. The challenge for forecasters is how to effectively use large numbers of model forecasts to reliably predict inherently rare, high-impact events days in advance.

Given the significant societal impacts severe thunderstorms and tornadoes pose, the authors are collaborating on methods to extend the range of forecasts for these events.

Here we begin to apply the longer range (up to 45 days) forecasts available from the CFSv2 to the daily severe weather prediction challenge. Our strategy for identifying model output of interest to forecaster is the following. An indication of potential predictability is when multiple consecutive forecasts exhibit similar outcomes, indicating that forecast outcomes are systematic responses to the evolving initial conditions. We would argue that it is reasonable to expect potential predictability to be a necessary, though not sufficient, requirement for achievable predictability and forecast skill. One approach we describe here reveals a relatively consistent potential predictability limit of around 7-days for daily-scale significant severe weather events occurring from late March through April 2014, when CFSv2 output is consolidated into single-day severe weather forecasts. Another approach, using run-cumulative information from CFSv2 long-lead forecasts to detect consistent anomalies in the forecasts, shows greater potential for skilful longer lead forecasts of severe weather activity. Robust verification of these approaches is beyond the scope of this paper. The concepts described, however, naturally lead to establishing a baseline climatology through application of reanalysis and reforecasts to further assess the predictability of regimes supportive of severe thunderstorms on longer time-scales (beyond the current one-week limit), including events occurring over multiple days.

OVERVIEW OF CFS

The National Centers for Environmental Prediction Climate Forecast System (CFSv2) became operational in March 2011 (Saha et al. 2014). The CFSv2 is a global spectral model with coupled ocean-sea-ice-land and atmosphere processes. The Climate Data Assimilation System version 2 (CDASv2; a real-time continuation of the Climate

Forecast System Reanalysis) is used to initialize operational CFSv2 runs (Saha et al. 2014). The CFSv2 has 64 vertical sigma-pressure hybrid layers and an equivalent horizontal grid spacing of approximately 100 km (T126).

CFSv2 output is available from 16 model runs per day. Four of those runs are forecasts out to nine months, three runs are forecasts for one season, and nine runs are 45-day forecasts. The CFSv2 parameters used in this study are taken from the ensemble mean of the four 0000 UTC model runs available in 6-hr timesteps out to 45 days. The four 0000 UTC model run ensemble membership consists of a control run and three perturbed members generated from differences between the current and previous initial model states and multiplied control factors (personal communication; Wanqiu Wang, NOAA).

While the range (resolution) of the CFSv2 may seem too long (coarse) for use in predicting the mesoscale aspects of severe thunderstorm events, the CFSv2 is capable of capturing climate signals (e.g. Kirtman 2009). Using time-lagged ensemble forecasts from this modeling system may allow the generation of potentially useful longer-range predictions of environments conducive to severe thunderstorms and tornadoes. These environments are defined by high levels of convective available potential energy (CAPE), strong low-level storm-relative helicity (SRH), and strong deep-layer vertical wind shear, or bulk wind difference (BWD; Doswell 1980; Brooks et al. 2003; Thompson et al. 2003, 2007; Grams et al. 2012). To depict synoptic-scale regimes potentially supportive of severe thunderstorms, we analyze daily averages (1200 UTC to 1200 UTC from 6-hr intervals) of a derived parameter, the supercell composite parameter

(SCP) that combines the fields of CAPE, SRH, and BWD from the CFSv2 over the contiguous United States (CONUS).

OVERVIEW OF CFSv2 SCP

The SCP (eq. 1) is a normalized index developed to define atmospheric environments with adequate instability, storm-relative helicity (SRH) and deep-layer vertical shear to support organized thunderstorms, usually in the form of supercells (Thompson et al. 2003; 2007). The formulation used here is slightly modified from the index defined by Thompson et al. (2003). Specifically, a 0-180 hPa layer “most-unstable” CAPE is taken directly from CFSv2 output and bulk shear is computed from the wind between the model’s 0-30 hPa layer and 500 hPa. SCP values ≥ 1 are associated with environments conducive to thunderstorm updraft persistence and rotation. The value of SCP is that it can be easily derived from near real-time high-resolution mesoanalysis data and from longer-range forecast grids, such as the CFSv2. Drawbacks include the SCP not being an explicit predictor of supercells and clearly not accounting for an array of other complex processes involved in the development of severe storms (Doswell and Schultz 2006). Nonetheless, the use of severe weather indices in defining severe thunderstorm climatologies, and in severe weather prediction, has been documented in a number of studies (Brooks et al. 2003; Tippett et al. 2012a). In particular, Tippett et al. (2012a) showed that monthly CFSv2 forecasts of a tornado environment index (derived from convective precipitation and SRH) showed significant correlations with the observed monthly number of tornadoes across the CONUS.

Eq. 1

1 $SCP = (CAPE / 1000 \text{ J kg}^{-1}) * (SRH / 50 \text{ m}^2 \text{ s}^{-2}) * (BWD / 20 \text{ m s}^{-1})$

2 Where:

3 CAPE = 0-180 mb convective available potential energy

4 SRH = 0-3 km storm-relative helicity

5 BWD = bulk-wind difference between 500 hPa and 0-30 hPa layer above ground u, v
6 winds

7
8 VISUALIZATION OF CFSv2 SCP GRID COUNTS

9 A challenge in utilizing CFSv2 output for long-range forecasting is the ability to analyze,
10 synthesize, and visualize the large amount of information available. The 45-day CFSv2
11 output is composed of a control run and three perturbed members with 6-hr timesteps.
12 In all, over 4000 individual forecasts per day are available from the system. One
13 approach to managing this amount of forecast information has been to consolidate 6-hr
14 forecasts of SCP into daily average SCP grid counts where the daily average is based
15 on a “convective day” (as defined by SPC) from 1200 UTC to 1200 UTC the following
16 calendar day. SCP forecasts can be further summarized by constructing the daily
17 averages from the four-member CFSv2 ensemble mean, and further utilizing only those
18 forecasts from the 0000 UTC model initialization. While this process does limit the
19 amount of CFSv2 forecast information from other runs, it is deemed a reasonable
20 approach for a proof of concept exercise. The relationship of 2014 CFSv2 forecasts of
21 convective day grid counts of average $SCP \geq 1$ to convective day tornado and hail
22 reports is shown in Fig. 1 for all verifying Day 1 CFSv2 forecasts. (Day 1 CFSv2
23 forecasts of 24-hr average SCP are comprised of 6-hr grids from 12-hr to 36-hr

forecasts and are used for verification.) There is a good association between forecast values of SCP and the number of tornado and hail reports.

Since December 2012, SPC forecasters have used an experimental web-based CFSv2 time lagged ensemble chart, or “Chiclet Chart”, to review 45-day forecasts of daily counts of the number of grid points with $SCP \geq 1$ from the 0000 UTC CFSv2 ensemble mean over the CONUS. Using this approach, grid count forecasts from successive CFSv2 runs can be viewed where each pixel or “chiclet” on the chart corresponds to one convective day and the color of the chiclet represents the grid count of the daily average $SCP \geq 1$ over a masked CONUS domain with 845 grid points. A similar display format, previously used in the context of ENSO and rainfall forecasts (Barnston et al. 2012; Tippett et al. 2012b; Tippett et al. 2015b), permits the visualization of multiple forecasts with the same valid time. The chart is constructed so that each successive CFSv2 run is stacked above prior runs, but staggered, so forecasts with identical valid times lie on the same x-axis coordinate (Fig. 2a). Vertical stripes of similar color indicate run-to-run consistency in $SCP \geq 1$ grid counts (i.e., similar forecasts in terms of the areal extent of environments conducive to supercell thunderstorms across the CONUS). Forecasters can further interrogate the information presented in the web-based CFSv2 Chiclet Chart when they mouse-over highlighted days to reveal CONUS maps of daily-averaged SCP grids (grid boxes and red contours), as well as the 24-hr convective quantitative precipitation forecasts (QPF, color-filled) to identify spatial patterns and locations where these fields overlap (Fig. 2b). By moving the mouse vertically along a column of highlighted days meeting SCP thresholds, the forecaster

1 can visualize CFSv2 run-to-run consistency in the maps of severe-storm environments,
2 magnitude of daily average SCP, and convective QPF.

3
4 The Chiclet Chart depicts forecast consistency of SCP ≥ 1 grid counts when similarly
5 colored chiclets appear in vertical sequences. Higher confidence can be given to severe
6 weather potential when both the consistency and the areal coverage of daily-averaged
7 SCP forecasts (from the CFSv2 ensemble mean) remain similar or increase as the valid
8 date approaches. However, many multi-day forecasts exist where a supportive regime
9 is shown by successive highlighted chiclets, or a decay in an earlier high-end signal
10 reappears at a later valid date, indicating uncertainty in the timing of events. Chiclet
11 maxima sloping up and to the left indicate a trend toward a faster system (earlier event
12 arrival), while maxima sloping up and to the right indicate a trend toward a slower
13 system (later event arrival). For the multiple-day events indicated on the Chiclet Chart
14 during this evaluation period, we will focus on the character of the forecasts from six
15 days in advance to the day of the severe weather event (Day 6 to Day 1 forecasts in
16 SPC parlance).

17
18 Another graph contained within the Chiclet Chart (Fig. 2, upper right) shows the forecast
19 range of SCP ≥ 1 grid counts (y-axis) from all available forecasts valid on the same
20 day, from Day 1 through Day 44 (x-axis). The quartile values of forecast grid counts are
21 shown. The range between minimum and maximum counts for the 10 most recent
22 forecasts is filled in gray, while the most recent forecast values are plotted as small
23 white circles. This additional information can aid the forecaster in interpreting trends in
24 CFSv2 output.

CFSv2 SCP EVALUATION FOR LATE MARCH AND APRIL 2014

Here we describe the character of CFSv2 daily CONUS forecasts for several severe weather events during the period from late March through April 2014. Of the 145 tornadoes reported in the CONUS during this period, 66 occurred on the four days reviewed here: 28 March, 3 April, 19 April, and 28 April. The most significant of these events occurred in late April when a multi-day tornado outbreak resulted in 84 tornadoes between 27 April and 30 April.

Correlation of CFSv2 SCP ≥ 1 Day 1 grid count forecasts with all other forecasts decreases as forecast lead time increases (Fig. 3, blue line). Correlation values plateau around the two-week mark and do not decrease further, likely a reflection of seasonality. The seasonal cycle is not removed in the correlation calculation. The decrease in forecast consistency is shown around the one-week mark (a drop below a 0.5 correlation value) in Fig. 3, and also by the lack of similarly colored vertical lines beyond days 5 through 7 on the Chiclet Chart for late March through 30 April 2014 (Fig. 2). To aid in delineating this transition from less consistent to more consistent forecasts, a sloped white line is drawn on subsequent Chiclet Charts evaluated below (Figs. 4, 6, 8, and 10).

Over 200 severe weather reports were plotted on the SPC report map valid for 28 March 2014 (Fig. 4, inset map). The potential for this particular event began to appear in CFSv2 forecasts around 21-22 March 2014. When viewing the evolution of the six forecasts leading up to 28 March, a consistent signal exists in both the areal coverage

1 and the magnitude of SCP ≥ 1 grid counts (Fig. 5). A slight westward shift in
2 convective QPF is evident as forecast lead time decreases, indicating a trend toward
3 slower eastward system evolution over time. The overall slower advance of this system
4 is also supported by the multi-day forecast (paired similarly colored chiclets) with 75
5 severe weather reports occurring primarily across the state of Missouri on 27 March
6 2014 (not shown).

7
8 The most active severe weather day of the first half of April 2014 occurred on the 3rd
9 day of the month with nearly 400 wind, hail and tornado reports. There were 13
10 tornadoes reported on this day, including one rated EF2. The CFSv2 forecasts again
11 provided indication of severe weather potential across a multiple-day period beginning
12 with forecasts initialized six to seven days in advance (Fig. 6). Strong consistency exists
13 in the Day 6 through Day 1 forecast maps valid for 3 April 2014 (Fig. 7). An additional
14 trend supporting greater confidence in a significant severe weather episode is the
15 steady increase in SCP ≥ 1 grid counts; from 100 in the Day 6 forecast to 135 in the
16 Day 2 forecast (Fig. 6 and 7). Only subtle changes are evident in the centroid of
17 the 24-hr convective QPF signal from one run to the next with this centroid also
18 corresponding closely to the centroid of severe weather reports for the event (Fig. 6,
19 inset map).

20
21 A weaker, single-day signal (lower grid count) from CFSv2 guidance is shown for the six
22 daily forecasts leading up to 13 April 2014 (Fig. 8). This event featured a mix of primarily
23 severe hail and wind reports, and six tornadoes rated no stronger than EF1. Forecast
24 maps reveal some possibility of a bi-modal event with the bulk of SCP ≥ 1 grids

1 counted across Texas, Arkansas and Louisiana; and a secondary corridor of SCP ≥ 1
2 evident over portions of the Midwest and Northeast (Fig. 9). The inconsistent nature of
3 the location of SCP ≥ 1 from one forecast to the next is consistent with greater
4 uncertainty in where severe weather may occur. Subjectively, this event is verified well
5 by the centroid of convective QPF in the CFSv2 forecasts. And, while the environment
6 for supercells may have existed and was accurately forecast by the CFSv2 along the
7 corridor from east of the Mississippi River to New England, a significant convective
8 precipitation signal was not present across this corridor. The lack of spatial overlap
9 between convective precipitation and SCP ≥ 1 in the forecasts could be viewed by the
10 forecaster as detrimental to confidence for more widespread severe weather; as was
11 the case for this event.

12
13 The most active and significant severe weather day of the month occurred on 28 April
14 2014. This was the second of a multi-day severe weather event, but the focus will be on
15 the forecasts leading up to this particular day. More than 50 tornadoes were reported
16 across six states, including eight tornadoes rated EF3 and one rated EF4. SCP ≥ 1
17 grid counts for this event begin to increase around 18 April 2014 (Day 11 forecast).
18 However, similar to the other events reviewed, a more consistent signal in SCP grid
19 count magnitude commences between Day 10 and Day 7 (Fig. 10). Also, similar to the 3
20 April 2014 event, forecast grid counts exhibit a steady increase; from 55 on Day 6 to
21 over 100 on Day 1 (Fig. 11). There is a distinct eastward shift in the area covered by
22 SCP ≥ 1 and the strong convective QPF signal around Day 3 is indicative of a faster
23 system motion/evolution. However, the overall co-location of high values of SCP and
24 convective QPF in forecasts from Day 3 to Day 1 correspond well with where significant

severe weather occurred. Using the maps in conjunction with the trends in $SCP \geq 1$ grid count/areal coverage can provide the forecaster with enhanced confidence in the magnitude of the severe weather event. While less significant, a smaller area where several severe wind and hail reports occurred across Missouri and Illinois was relatively well indicated by $SCP \geq 1$ in the CFSv2 maps starting with the Day 5 forecast for this event.

UTILITY FOR WEEK TWO AND BEYOND

Generally beyond a lead time of seven days, the CFSv2 exhibits more run-to-run variability, providing a less consistent signal for an event (i.e. no vertical stripe on the chart). However, if $SCP \geq 1$ grid counts are accumulated from run to run, better signals emerge for some events beyond the first week. These events demonstrate the benefit of using past CFSv2 runs in a time-lagged ensemble approach. To illustrate this utility, the lead time is switched to the y-axis, with each run of the CFSv2 along parallel diagonals (Fig. 12). Although there are few vertical stripes beyond day 10, there is a clear indication of the seasonality of severe weather. Taking a running (with respect to decreasing lead time) sum of all forecast $SCP \geq 1$ grid counts verifying on the same day (Fig. 13) shows the strong seasonality of CFSv2 ensemble-mean of accumulated $SCP \geq 1$, with the largest accumulated values peaking during June over the CONUS. Embedded in the plot are vertical spikes where runs of the CFSv2 have exhibited particularly favorable conditions (compared to a two-week window) for severe weather over multiple runs (Fig. 14). Removing the mean of a two-week window around each forecast day produces a forecast anomaly plot that reveals vertical stripes where forecast SCP counts have accumulated from multiple model runs (Fig. 15), indicating a

1 relatively favorable severe weather environment. Note that diagonal features
2 correspond to single forecast runs, and while they are present at long lead times, the
3 accumulation method tends to smooth out run-to-run variability. The correlation of all
4 positive anomaly forecasts to Day 1 forecasts of positive anomaly (used as verification)
5 appears to extend the consistency in these forecasts to at least 15 days (Fig. 3, green
6 line). This approach nearly doubles the period of useful forecasts (correlation values
7 above 0.5) compared to the single day SCP grid count forecasts used in the Chiclet
8 Chart.

9
10 Figure 16 provides subjective verification of positive anomaly forecasts for the period 8
11 January through 14 May 2014. (This portion year is used to assist in visualization. The
12 underlying chart of positive anomalies is the same as shown in Fig. 15, only zoomed to
13 1 January through 14 May 2014. The first week of January 2014 data is used in
14 computing the mean of a two-week window around each forecast day so that SCP
15 positive anomaly forecasts commence on 8 January 2014.) Semi-transparent gray bars
16 plotted over the colored positive anomaly forecasts indicate days with a significant
17 number of observed hail and/or tornado events. Bars extending to half the y-axis in Fig.
18 16 are days with a total number of severe hail and tornado events exceeding the daily
19 mean (18) for the period 1 January through 14 May, 2014, but not exceeding one
20 standard deviation above the mean. Bars fully encompassing the y-axis are days with a
21 total number of severe hail and tornado events exceeding one standard deviation above
22 the mean (76 reports).

1 Weak false alarms appear in the positive anomaly forecasts on 11 and 14 January
2 when no significant severe weather was reported. More substantial false alarms appear
3 from 3 through 5 February when normalized values in the range of 20 to 30 begin to
4 appear in 5 to 7 day forecasts but no severe weather meeting our criteria are indicated.
5 The stronger positive anomalies occurring on 21 and 22 February coincide with a
6 couple of days of above average severe weather (semi-transparent gray bars extending
7 to half the y-axis in Fig. 16). The CFSv2 forecast signal for these two days begins to
8 strengthen around 20 to 22 days in advance, fades, then returns in the 5 to 10 day
9 forecast range. These events are also followed by three days (22 through 24 February)
10 with relatively strong positive anomaly forecasts but no severe weather indicated.
11
12 The multiple-day severe weather events observed around the beginning of April and
13 reviewed above using the Chiclet Chart also show up well using the positive anomaly
14 forecast approach. The 2 through 4 April events are characterized by less lead time
15 than the 28 and 29 March events (27 March, while being an above average severe
16 weather day, was a missed forecast). The greatest positive anomalies of the entire year
17 coincide with the significant severe weather events occurring at the end of April 2014.
18 These events are preceded by a couple of above average severe weather days that are
19 poorly forecast (gray bars with no underlying color on 21 and 23 April). With the
20 exception of 26 April, positive anomaly forecasts for the period 24 through 30 April all
21 verified with above or much above normal severe weather activity. The greatest
22 normalized positive anomaly of 100 occurs on 28 April, a day with the highest total
23 number of significant tornadoes in 2014 (21 tornadoes rated \geq EF2). Positive anomaly
24 forecasts for these active severe weather days at the end of April begin to appear

1 around day 40 but values are not substantially discernable from other active and false
2 alarm days until around day 21, three weeks prior to the events, when positive anomaly
3 values around 30 are indicated. Large anomalies can begin at these long forecast lead
4 times but can also fade as the verification date approaches. However, in the case of late
5 April, the amplitude of the positive anomaly increases, indicating continuing support
6 from subsequent forecasts leading up to the event.

7
8 The positive anomaly forecast method also appears to exhibit skill in depicting the lack
9 of supportive environments for severe weather. This is shown best during the period 1
10 through 6 May when the lack of any severe weather events of significance corresponds
11 well with near 0 value anomaly forecasts. The positive anomaly signal returns and
12 persists from 7 through 13 May and coincides well with a string of significant severe
13 weather days (gray bars extending along the entire y-axis in Fig. 16). A number of these
14 forecasts exhibit relatively short lead times of five to seven days, or generally weak
15 long-lead positive anomaly forecasts. The final day of the time series shown in Fig. 16 is
16 14 May, a day with a significant number of severe weather events but a fading signal in
17 the positive anomaly forecast.

18
19 These examples demonstrate that while consecutive daily forecasts may exhibit large
20 inconsistency at long lead times (Fig. 12), there may still be utility from the CFSv2
21 forecasts regarding favorable severe weather environments beyond one week by
22 accumulating grid counts of $SCP \geq 1$, and applying a time averaging technique to
23 derive forecast anomalies as described here.

CONCLUSIONS AND CONTINUING RESEARCH

The Chiclet Chart and accompanying maps of SCP areal coverage demonstrate the predictive skill of the CFSv2 for identifying severe weather events based on environments with large CAPE and strong vertical wind shear, as indicated by SCP values ≥ 1 . For days reviewed during March-April 2014, the CFSv2 showed consistent forecasts of SCP coverage beginning around seven days before the severe weather events.

Once the CFSv2 indicates a possible upcoming event, further investigation is needed in order to ensure skillful severe weather prediction. Ensemble averaging across several runs may help increase confidence and lead time. In addition, synoptic and larger-scale pattern recognition within a CFSv2 ensemble mean is important for evaluating severe weather potential. Other environmental factors should also be considered, as well as parameter normalizations calibrated specifically to CFSv2 climatology. For example, high SCP environments can accompany both capped days with no convection, and uncapped days with widespread interfering convective cells. Considering convective inhibition (CIN) and convective QPF along with SCP should also provide the forecaster with additional information and confidence in making extended range forecasts for severe convection.

Beyond seven days, run-to-run consistency decreases substantially. The patterns observed on the Chiclet Chart in this situation are comprised of more horizontal streaks rather than vertical streaks. The horizontal streaks are indicative of periods of favorable environmental conditions for severe weather on a synoptic time scale. These regimes

1 tend to be characterized by positive feedback, such that the synoptic pattern favorable
2 for strong convection is repeated. As a result, consecutive model runs can exhibit
3 drastic differences from week-two and beyond.

4
5 Despite the run-to-run variability, signals in the extended range can be extracted by
6 integrating the SCP ≥ 1 grid counts across all forecast runs. This approach reveals
7 long vertical spikes on the chart where past runs of the CFSv2 produced greater
8 coverage of SCP ≥ 1 for the same day. This visualization method serves as a
9 supplement to the Chiclet Chart by highlighting days at extended lead times that require
10 attention in future forecast runs. Following the implementation of these real-time
11 products, the use of the visualization methods presented here will be expanded to
12 include different forecast models and forecast variables.

14 ACKNOWLEDGEMENTS

15 This study was supported by NOAA award NA14OAR4310185, the Office of Naval
16 Research award N00014-12-1-091 and a Columbia University Research Initiatives for
17 Science and Engineering (RISE) award. S. Lillo's contribution was supported under
18 NOAA-OAR-CPO grant 2014-2003692. The views expressed herein are those of the
19 authors and do not necessarily reflect the views of NOAA or any of its sub-agencies.
20 We wish to thank Israel Jirak of SPC for his thorough review of the manuscript prior to
21 submission and three reviewers for further constructive comments and suggestions to
22 improve this work.

24 AFFILIATIONS: Carbin - NOAA/National Weather Service Storm Prediction Center,
25 Norman, Oklahoma; Lillo - University of Oklahoma, Cooperative Institute of Mesoscale
26 Meteorological Studies (CIMMS), Norman, Oklahoma; Tippett - Department of Applied

1 Physics and Applied Mathematics, Columbia University, New York, New York and
2 Center of Excellence for Climate Change Research, Department of Meteorology, King
3 Abdulaziz University, Jeddah, Saudi Arabia; Brooks - NOAA/OAR/National Severe
4 Storms Laboratory, Norman, Oklahoma.

5

6

7

REFERENCES

Allen, J. T. , M. K. Tippett, and A. H. Sobel, 2015: Influence of the El Niño/Southern Oscillation on tornado and hail frequency in the United States. *Nat. Geosci.*, **8**, 278–283.

Barnston, A. G., M. K. Tippett, M. L. L’Heureux, S. Li, and D. G. DeWitt, 2012: Skill of real-time seasonal ENSO model predictions during 2002–2011. Is our capability increasing? *Bull. Am. Meteor. Soc.*, **93**, 631–651.

Brooks, H. E., J. W. Lee, and J. P. Craven, 2003: The spatial distribution of severe thunderstorm and tornado environments from global reanalysis data. *Atmos. Res.*, **67–68**, 73–94.

Doswell, C. A. III, 1980: Synoptic-scale environments associated with high plains severe thunderstorms. *Bull. Amer. Meteor. Soc.*, **61**, 1388–1400.

Doswell, C. A. III, and D. M. Schultz, 2006: On the use of indices and parameters in forecasting severe storms. *Electronic J. Severe Storms Meteor.*, **1**, 1–14.

Grams, J. S., R. L. Thompson, D. V. Snively, J. A. Prentice, G. M. Hodges, and L. J. Reames, 2012: A climatology and comparison of parameters for significant tornado events in the United States. *Wea. Forecasting*, **27**, 106–123.

Kirtman, B. P. and M. Dughong, 2009: Multimodel Ensemble ENSO Prediction with CCSM and CFS. *Mon. Wea. Rev.*, **137**, 2908–2930.

Saha, S. and Coauthors, 2014: The NCEP Climate Forecast System Version 2. *J. Climate*, **27**, 2185–2208.

1

2 Thompson, R. L., R. Edwards, J. A. Hart, K. L. Elmore, and P. Markowski, 2003: Close

3 proximity soundings within supercell environments obtained from the Rapid Update

4 Cycle. *Wea. Forecasting*, **18**, 1243–1261.

5

6 Thompson, R. L., C. M. Mead, and R. Edwards, 2007: Effective storm-relative helicity

7 and bulk shear in supercell thunderstorm environments. *Wea. Forecasting*, **22**, 102–

8 115.

9

10 Tippett, M. K., A. H. Sobel, and S. J. Camargo, 2012a: Association of U.S. tornado

11 occurrence with monthly environmental parameters, *Geophys. Res. Lett.*, **39**, L02801.

12

13 Tippett, M. K., A. G. Barnston, and S. Li, 2012b: Performance of recent multi-model

14 ENSO forecasts. *J. Appl. Meteor. Climatol.*, **51**, 637–654.

15

16 Tippett, M. K., A. H. Sobel, S. J. Camargo, and J. T. Allen, 2014: An empirical relation

17 between U.S. tornado activity and monthly environmental parameters. *J. Climate*, **27**,

18 2983–2999.

19

20 Tippett, M. K., J. T. Allen, V. A. Gensini, and H. E. Brooks, 2015a: Climate and

21 hazardous convective weather, *Curr. Clim. Change Rep.*, **1**, 60–73.

22

23 Tippett, M. K., M. Almazroui, and I.-S. Kang, 2015b: Extended-range forecasts of areal-

24 averaged Saudi Arabia rainfall. *Wea. Forecasting*, **30**, 1090–1105.

25

26

- 1 World Meteorological Organization Bulletin, 2007: Seasonal Tropical Cyclone
- 2 Forecasts. [Available online at <http://www.wmo.int/pages/prog/arep/wwrp>
- 3 [/tmr/documents/seasonaltcforecasts.pdf](http://www.wmo.int/pages/prog/arep/wwrp/tmr/documents/seasonaltcforecasts.pdf).]
- 4

FIGURE CAPTIONS LIST

Fig. 1. The relationship of all 2014 Day 1 CFS forecasts of convective day grid counts of average SCP ≥ 1 (x) to convective day tornado and hail reports (y). Day 1 CFSv2 forecasts of 24-hr average SCP are comprised of 6-hr grids from 12-hr to 36-hr forecasts and are used for verification. The coefficient of determination of 0.58 and 95 percent confidence interval (shaded) are shown.

Fig. 2. a) CFS SCP Chiclet Chart for the period from 18 March to 30 April, 2014. b) Example of mouseover on a Day 2 chiclet with corresponding pop-up map valid on 3 April 2014.

Fig. 3. Blue line depicts the correlation of 2014 CFSv2 SCP Day 1 SCP grid counts with all other CFS grid count forecasts from Day 44 through Day 1 ($r = 1$). Green line depicts a similar comparison but using time-lagged accumulation of SCP grid counts, and removing the 2-week running mean centered on each forecast day, to derive positive anomaly forecasts.

Fig. 4. Forecasts of SCP grid count (Day 6 to Day 1) and resulting SPC storm reports (map, upper left) valid 28 March 2014.

Fig. 5. Forecast maps of SCP grid count (contours) and convective QPF (colors) from Day 6 to Day 1 valid 28 March 2014.

Fig. 6. Same as Fig. 4, except for 3 April 2014.

Fig. 7. Same as Fig. 5, except for 3 April 2014.

Fig. 8. Same as Fig. 2, except for 13 April 2014.

Fig. 9. Same as Fig. 5, except for 13 April 2014.

Fig. 10. Same as Fig. 2, except for 28 April 2014.

Fig. 11. Same as Fig. 3, except for 28 April 2014.

Fig 12. All 2014 CFSv2 forecasts of SCP ≥ 1 grid counts from day 44 to day 1 (from 00 UTC CFSv2 ensemble mean).

Fig. 13. Normalized running sum (over lead) of all forecast SCP ≥ 1 grid point counts verifying on the same day produces a curve of CONUS-wide SCP.

Fig. 14. Normalized two-week average window centered on each daily forecast of summed SCP grid counts.

Fig. 15. Normalized cumulative grid count positive anomaly forecast. The result of subtracting the data in Fig. 14 from that in Fig. 13.

Fig. 16. Underlying colored chart is same as Fig. 15 but zoomed to period 1 Jan to 14 May, 2015. Overlying semi-transparent gray vertical bars are days with above average (half-bar) or more than one standard deviation above average (full-bar) severe hail and tornado reports. The first week of January 2014 data is used in computing the mean of a two-week window so that SCP positive anomaly forecasts commence on 8 January 2014.

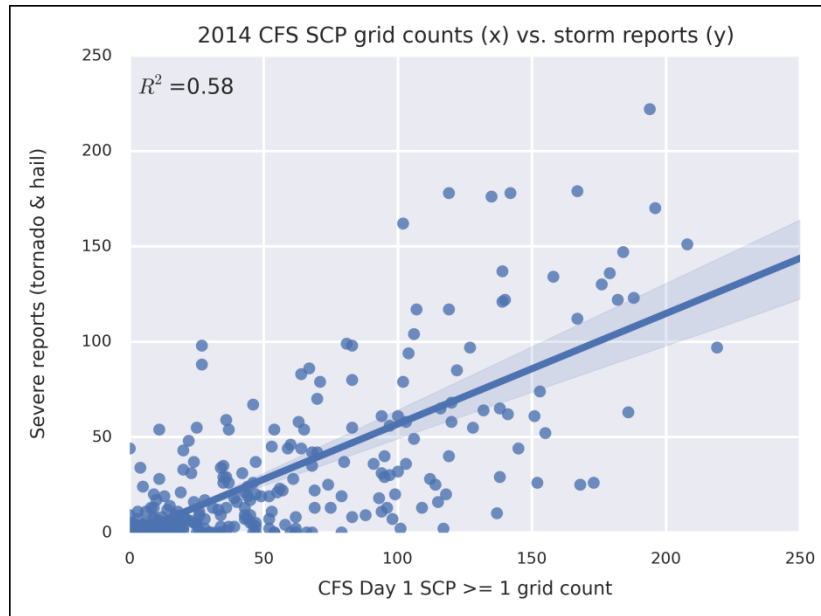


Fig. 1. The relationship of all 2014 Day 1 CFS forecasts of convective day grid counts of average SCP \geq 1 (x) to convective day tornado and hail reports (y). Day 1 CFSv2 forecasts of 24-hr average SCP are comprised of 6-hr grids from 12-hr to 36-hr forecasts and are used for verification. The coefficient of determination of 0.58 and 95 percent confidence interval (shaded) are shown.

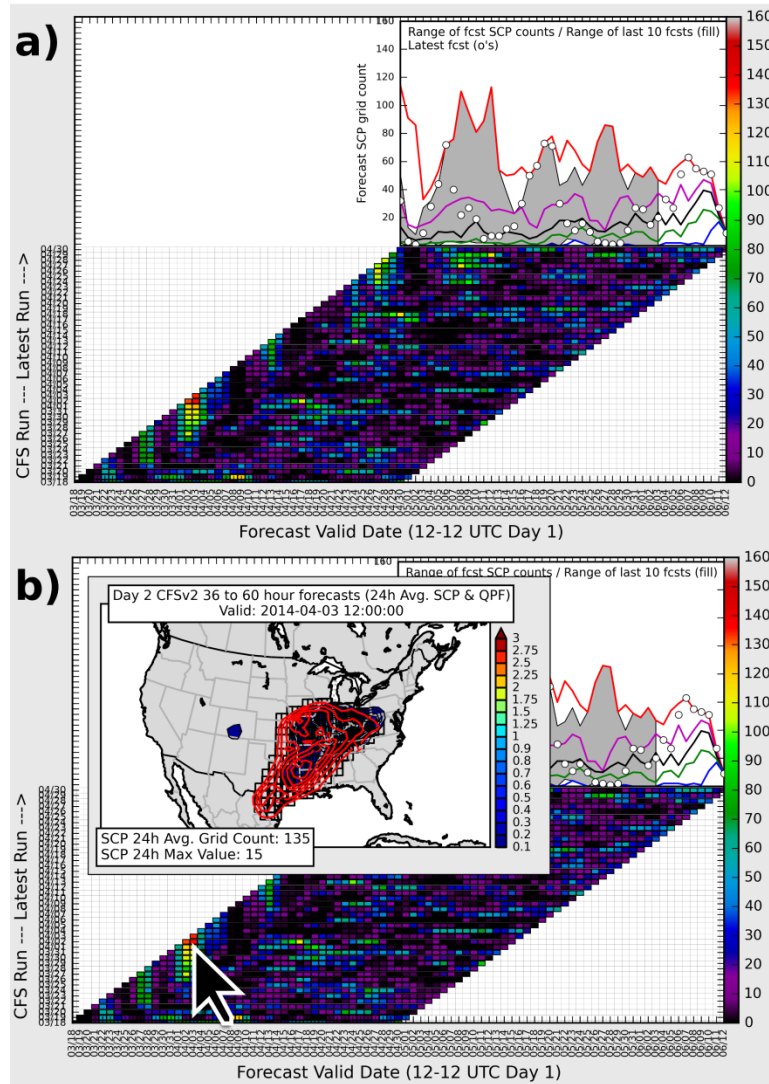


Fig. 2. a) CFS SCP Chiclet Chart for the period from 18 March to 30 April, 2014. b) Example of mouseover on a Day 2 chiclet with corresponding pop-up map valid on 3 April 2014.

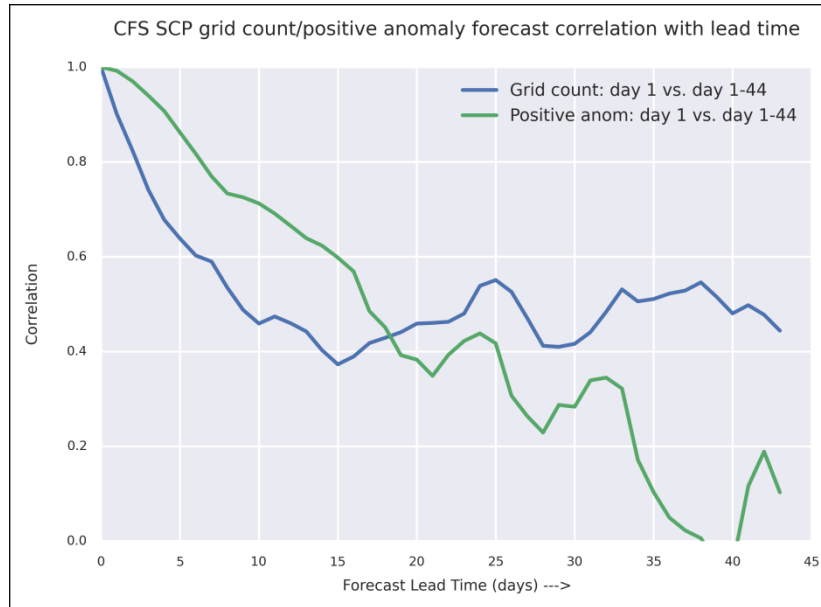


Fig. 3. Blue line depicts the correlation of 2014 CFSv2 SCP Day 1 SCP grid counts with all other CFS grid count forecasts from Day 44 through Day 1 ($r = 1$). Green line depicts a similar comparison but using time-lagged accumulation of SCP grid counts, and removing the 2-week running mean centered on each forecast day, to derive positive anomaly forecasts.

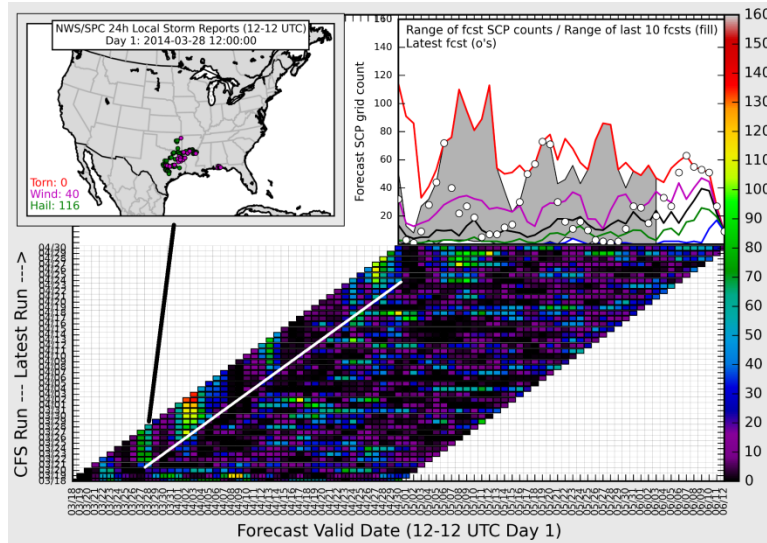


Fig. 4. Forecasts of SCP grid count (Day 6 to Day 1) and resulting SPC storm reports (map, upper left) valid 28 March 2014.

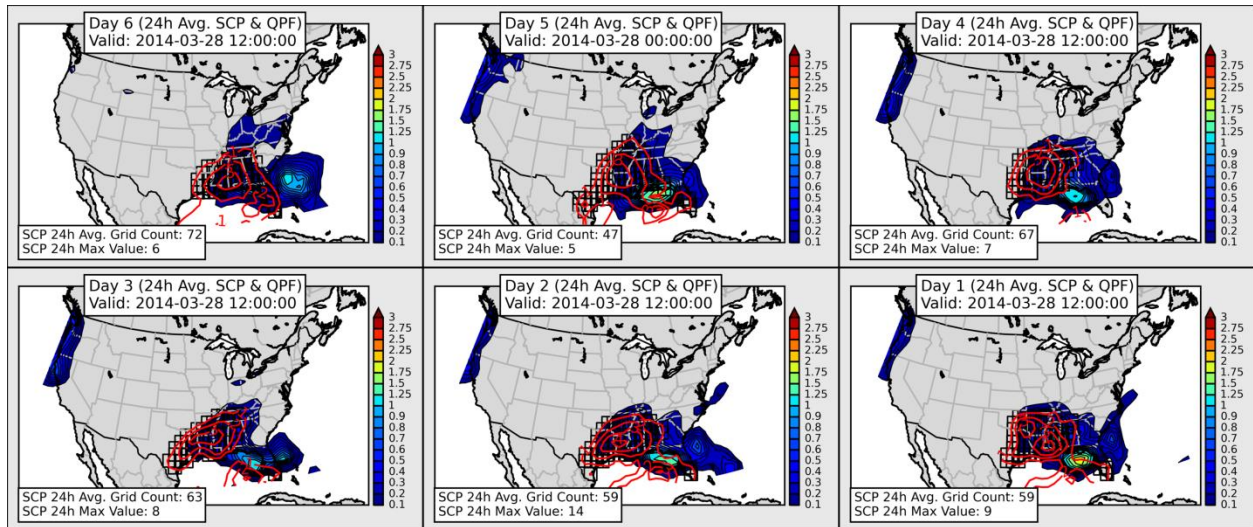


Fig. 5. Forecast maps of SCP grid count (contours) and convective QPF (colors) from Day 6 to Day 1 valid 28 March 2014.

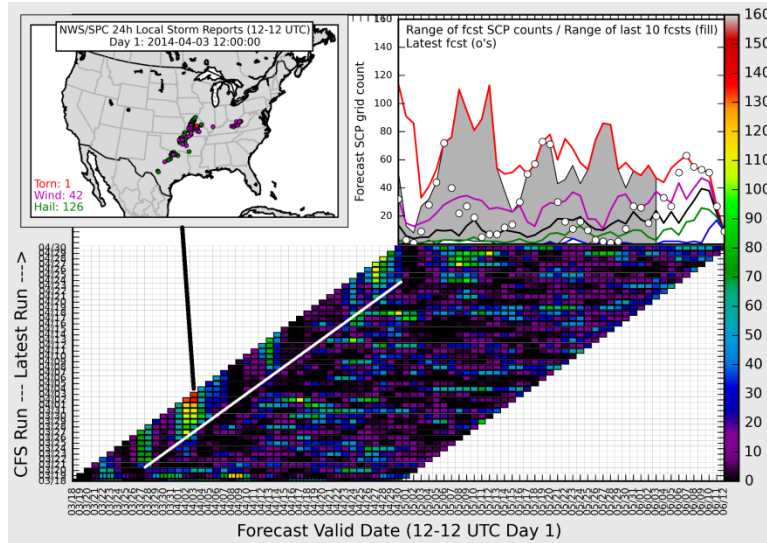


Fig. 6. Same as Fig. 4, except for 3 April 2014.

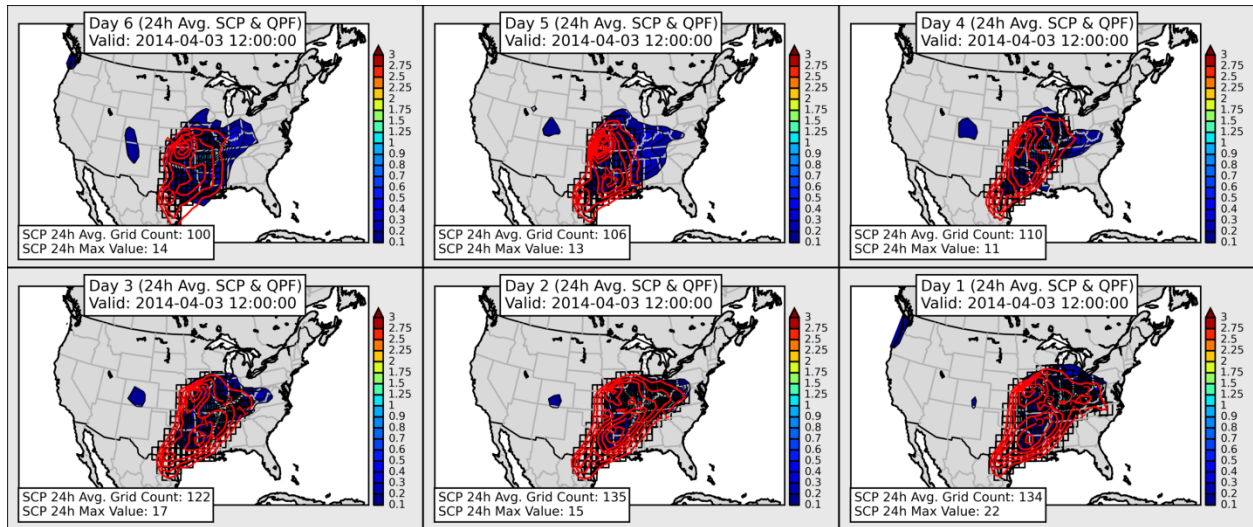


Fig. 7. Same as Fig. 5, except for 3 April 2014.

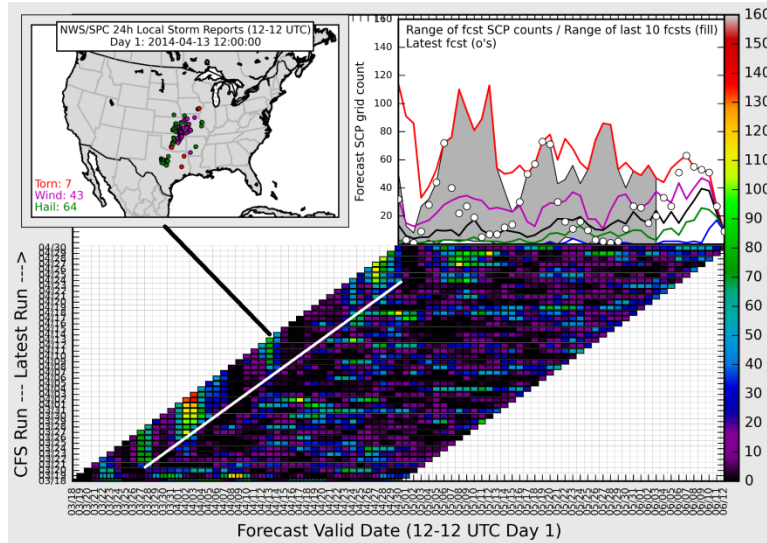


Fig. 8. Same as Fig. 2, except for 13 April 2014.

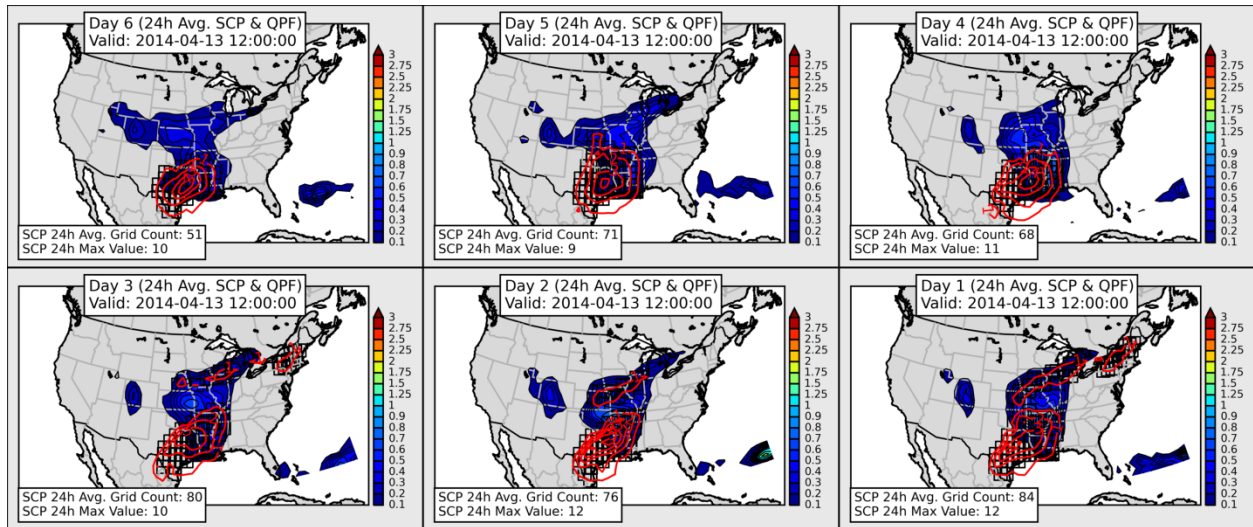


Fig. 9. Same as Fig. 5, except for 13 April 2014.

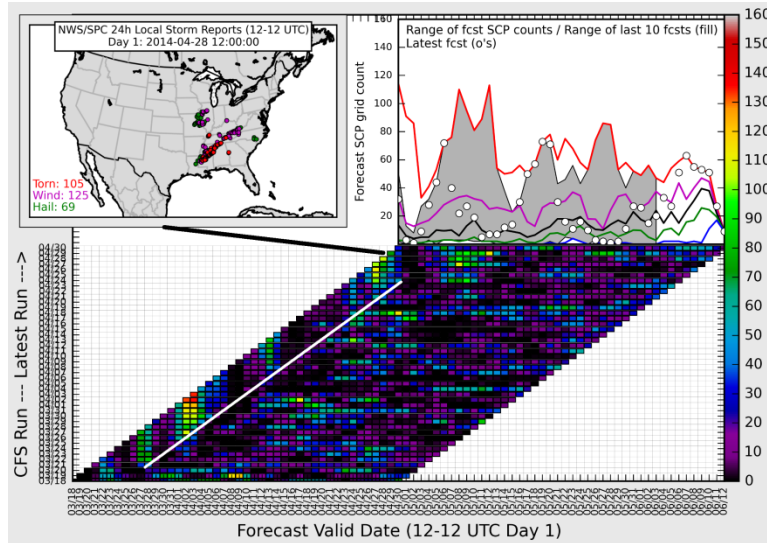


Fig. 10. Same as Fig. 2, except for 28 April 2014.

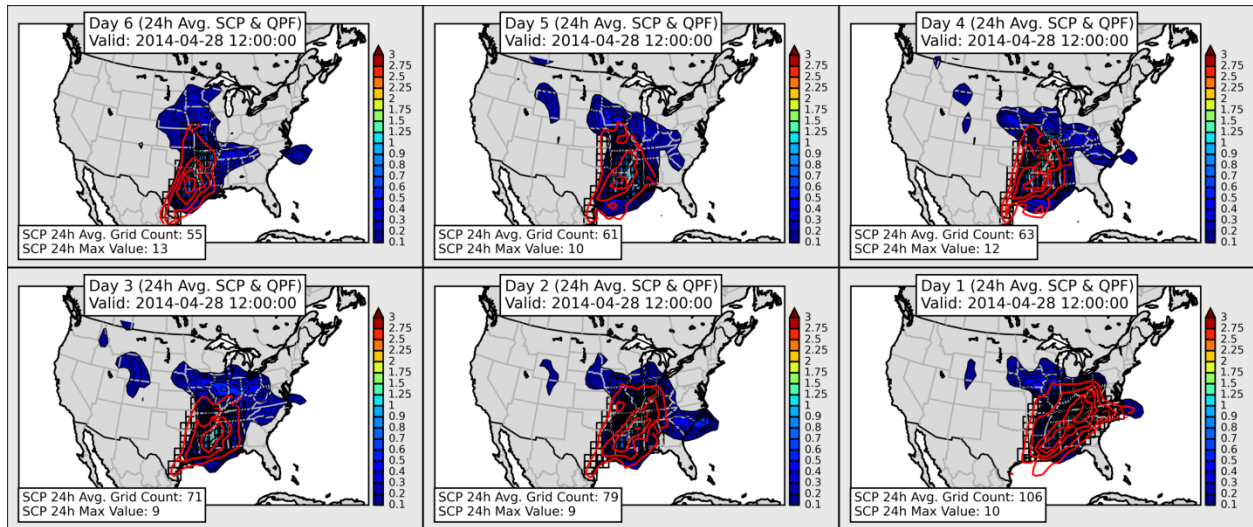


Fig. 11. Same as Fig. 3, except for 28 April 2014.

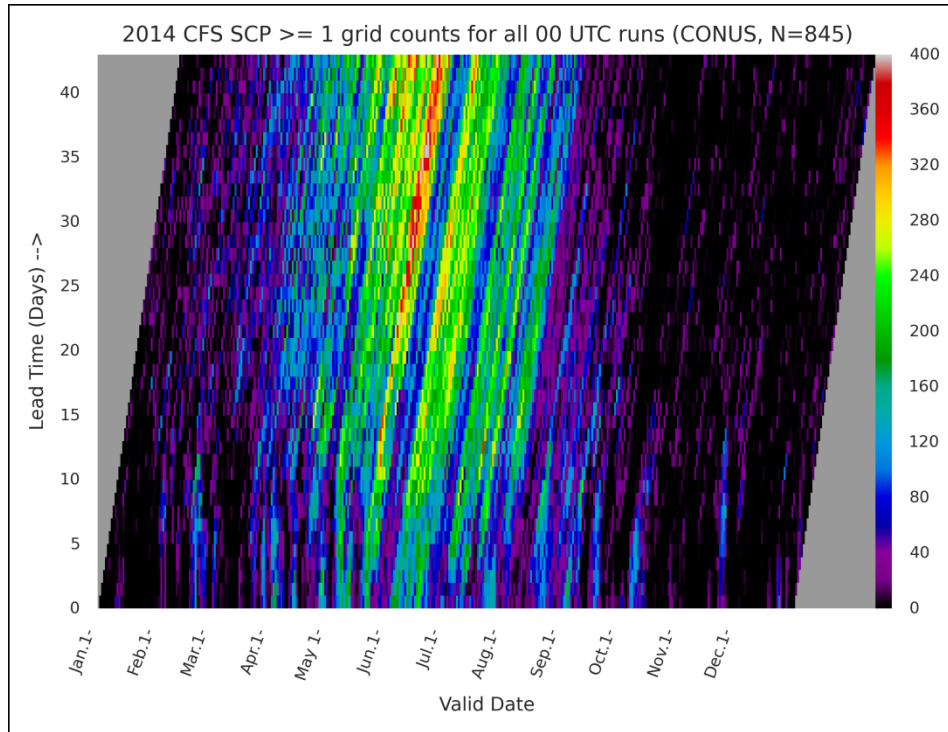


Fig 12. All 2014 CFSv2 forecasts of SCP ≥ 1 grid counts from day 44 to day 1 (from 00 UTC CFSv2 ensemble mean).

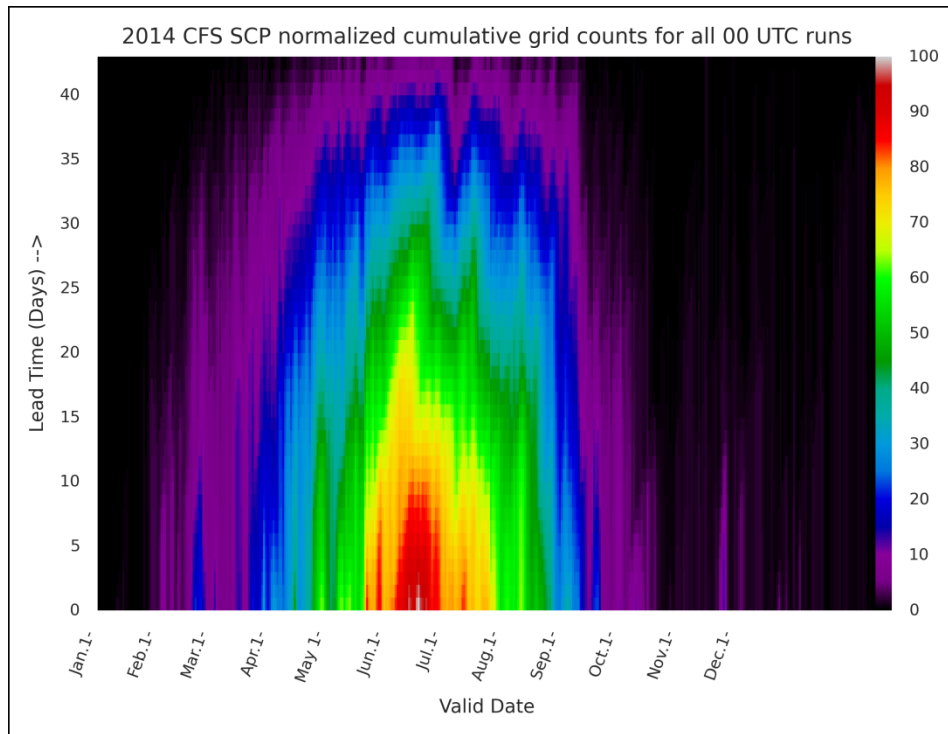


Fig. 13. Normalized running sum (over lead) of all forecast SCP ≥ 1 grid point counts verifying on the same day produces a curve of CONUS-wide SCP.

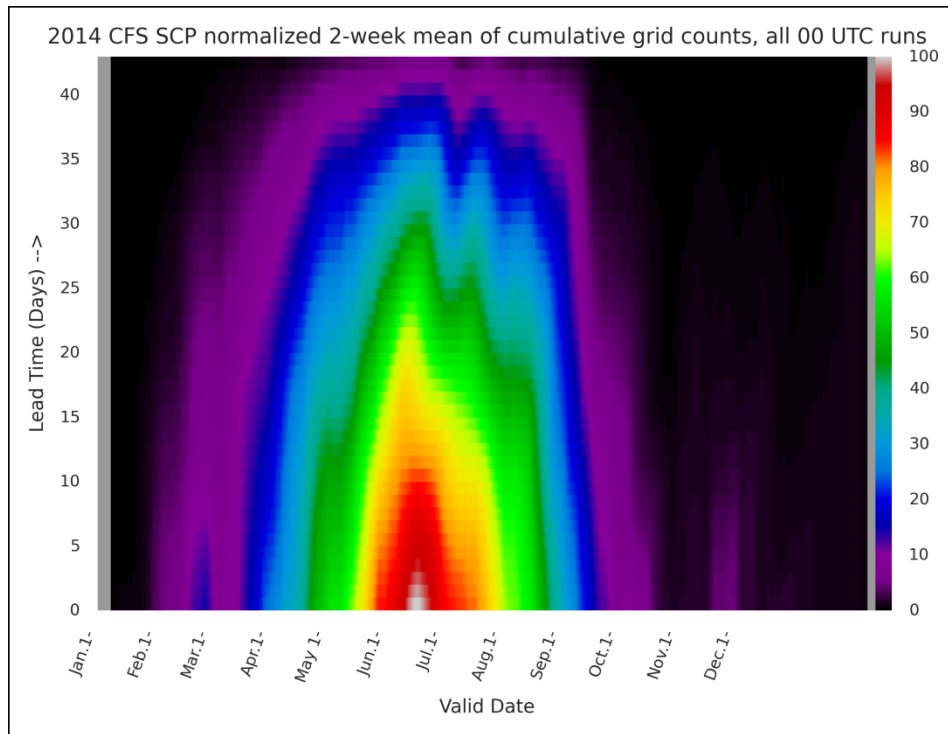


Fig. 14. Normalized two-week average window centered on each daily forecast of summed SCP grid counts.

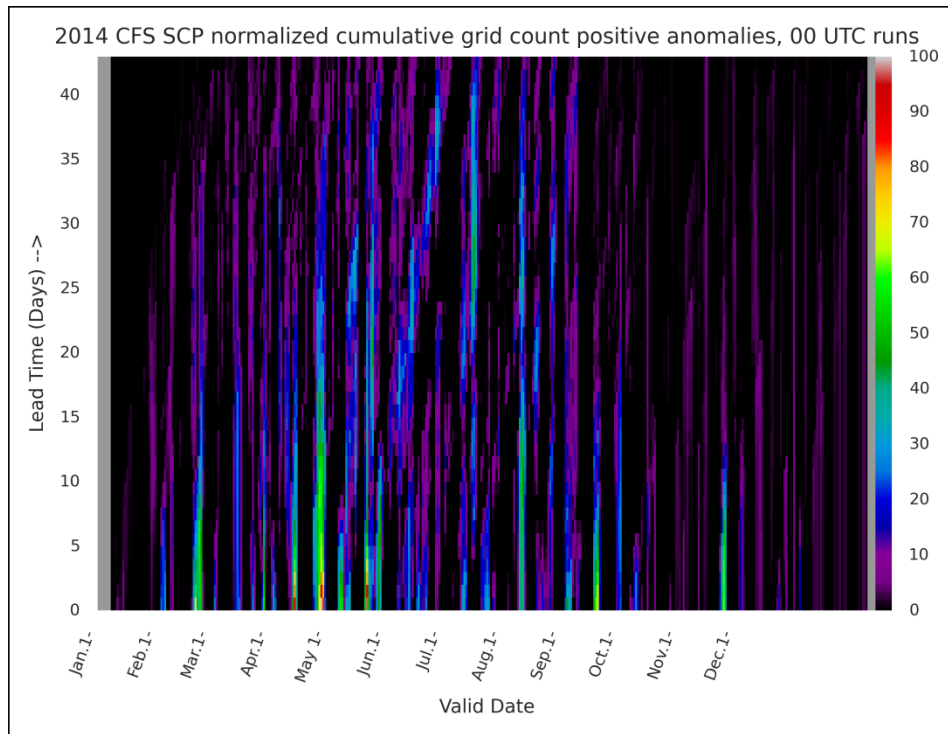


Fig. 15. Normalized cumulative grid count positive anomaly forecast. The result of subtracting the data in Fig. 14 from that in Fig. 13.

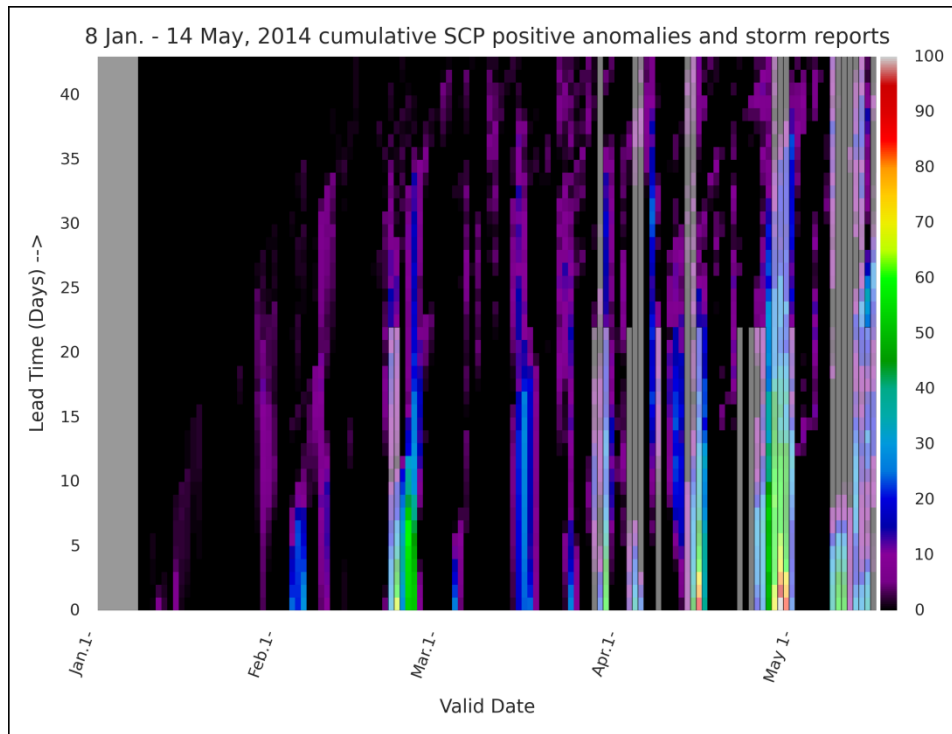


Fig. 16. Underlying colored chart is same as Fig. 15 but zoomed to period 1 Jan to 14 May, 2015. Overlying semi-transparent gray vertical bars are days with above average (half-bar) or more than one standard deviation above average (full-bar) severe hail and tornado reports. The first week of January 2014 data is used in computing the mean of a two-week window so that SCP positive anomaly forecasts commence on 8 January 2014.